Low frequency observations of high redshift galaxies

Jayaram N. Chengalur

NCRA-TIFR, Pune University Campus, Ganeshkhind, Pune 411 003, India

Although our understanding of the evolution of the stellar population of galaxies has improved dramatically in the recent past, our understanding of the evolution of the neutral atomic gas content in star forming galaxies remains limited. This is largely because of the sensitivity limit of the current generation of radio telescopes. The scenario is changing however, both because of new instrumentation and deeper integrations with the existing telescopes. In this article, I review the current status of, and future prospects for, low radio frequency observations of gas in high redshift galaxies. The indications are that the community is moving from an era of fasting to an epoch of feasting.

Keywords: Galaxies, evolution, hydrogen radio-astronomy.

WHILE there is a broad consensus that galaxies (or to be more precise galactic halos) formed through hierarchical merging, the fate of the gas in collapsed structures is far less well understood. The general outline of the current model for galaxy formation was established several decades ago (e.g. ref. 1). Density perturbations in the dissipationless dark matter grow due to gravitational instabilities. In the CDM or ΛCDM models, the growth is bottom up, i.e. small objects virialize first and in turn merge to form larger structures. The baryonic material is carried along by the gravity of the dark matter, cools and settles in the centre of the dark matter halos. While the dynamics of the dark matter can be fairly accurately captured in numerical simulations, the physics of the baryonic matter is much more complex and poorly understood. Observational constraints on the redshift evolution of the gas content of galaxies are hence of particular importance. In this review I focus on the role that low frequency radio spectral line observations play in our understanding of the evolution of gas in normal galaxies.

The vast majority of low frequency spectral line observations are of the redshifted hydrogen hyperfine line (with a rest wavelength of ~21 cm). Another set of spectral lines that have been gaining importance are the 18 cm lines ('Λ-doubling') from the OH molecule. These can be detected in emission in OH megamaser galaxies[2] but are also being increasingly detected in absorption from the ISM of normal galaxies at high redshift. The OH emission in megamaser galaxies traces the intense star formation in their dense central regions; these galaxies are typically undergoing a starburst and are often merging[3]. As such, OH megamaser emission could be used as a tracer for the evolution of the star-burst phenomena, and possibly the role of mergers in galaxy formation. OH absorption, on the other hand is a tracer of gas in normal galaxies, which is the focus of this review.

There are two complementary approaches to studying HI in galaxies at medium and high redshifts. The first approach is based on observations of the gas in emission. This yields information on the total gas content and large scale dynamics of the gas. On the other hand, at current sensitivities, observations are limited to relatively small redshifts. Only a very limited number of galaxies with $z \lesssim 0.03$ have been observed in the HI 21 cm line with synthesis telescopes. Even at these redshifts, one is often limited to studying only the most massive systems. The other approach is to observe the gas in absorption against a distant radio source. In this case, even at current sensitivities one can detect gas out to cosmologically large redshifts. On the other hand, the observations trace the gas only along one or at most a few limited different lines of sight, and the total gas content and global kinematics are often poorly constrained. The first two sections of this review highlight these two different approaches. In the final section, I look ahead to observations that could be done with the upcoming new radio facilities, and the future Square Kilometer Array (SKA).

Emission measurements

As mentioned above, the most widely observed low radio frequency spectral lines from external galaxies are the HI 21 cm line and the OH lines at 18 cm. The HI line is particularly an interesting one, because (1) it traces a major component of the neutral ISM of galaxies, and (2) because its optical depth is in general small, allowing one to directly measure the total gas content as well as large scale kinematics. Unfortunately, at the current sensitivity limits, it is not easy to observe statistically large samples of galaxies at redshifts beyond ~0.06. Thus, the best existing radio emission line estimate of the gas density of the universe (Ω_{gas}) is based on observations of galaxies[4] with $z \lesssim 0.04$. This is a very small redshift interval com-

e-mail: chengalur@ncra.tifr.res.in

pared to that at which galaxy evolutionary effects are expected to be important. For example (see refs 5–7), it is now well established that the star formation rate in galaxies was much larger at $z \sim 1$ than at the current epoch. This can be clearly seen in Figure 1 (taken from ref. 7), which shows the evolution of the star formation rate density with redshift. In contrast, the evolution of the gas content of galaxies with redshift, i.e. $\Omega_{gas}(z)$ is relatively poorly constrained (see Figure 2).

In the recent past however, there have been several attempts to observe targeted samples of galaxies at somewhat higher redshifts. Zwaan *et al.*[9] used the WSRT to observe HI in galaxies in the $z \sim 0.176$ cluster A2218. Clusters of galaxies are often favoured targets for deep HI observations, in part because the large space density of galaxies in clusters allows one to observe many galaxies in a single pointing and frequency setting. Another major driver for these observations is to understand the evolution of galaxies in clusters. A variety of mechanisms (e.g. interaction with the inter cluster medium[10,11], tidal interactions with other galaxies[12,13] are expected to lead to a much more rapid evolution of galaxies in clusters as compared to galaxies in the field. Direct evidence for the profound effect on the galactic ISM when a galaxy falls into a cluster comes from imaging of the HI disks of galaxies in the nearby Virgo cluster. Earlier VLA observations[14] of the central galaxies in this cluster showed that they had truncated disks and sharp edges on the side towards the centre of the cluster. Recent high sensitivity observations show, in addition, long tails that point away from the centre of the cluster (Figure 3, ref. 15) reinforcing the idea that the galactic ISM is being swept away as the galaxy falls into the cluster.

While clusters are interesting to study because of the interaction between the intra-cluster medium and the ISM of the infalling galaxies, precisely for these reasons, cluster galaxies tend to be deficient in HI. From the morphology-density relation[16] one would anyway expect that the majority of galaxies in the cluster core have early morphological types and are hence inherently gas poor. Apart from this, it is well established that, in clusters, even those galaxies with late morphological types have systematically lower gas content than similar galaxies in the field[17]. For example, Solanes *et al.*[18] found that two-thirds of the clusters in their sample had a deficiency of hydrogen in the galaxies near the cluster centre. Galaxies lying up to 2 Abell radii from the centre were found to be HI poor. Deep observations of fields containing galaxy clusters are hence more likely to detect HI from galaxies in groups in the periphery of the cluster than in the cluster itself. In the case of A2218, after a total observing time of 36×12 h (split across two different frequency set-

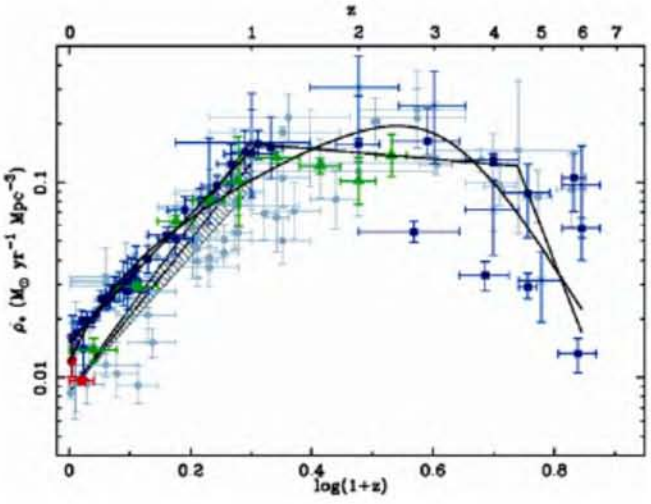

Figure 1. The evolution of the star formation rate density as a function of redshift (from ref. 7). The star formation rate has been measured using a variety of tracers, from radio to UV. See ref. 7 for more details.

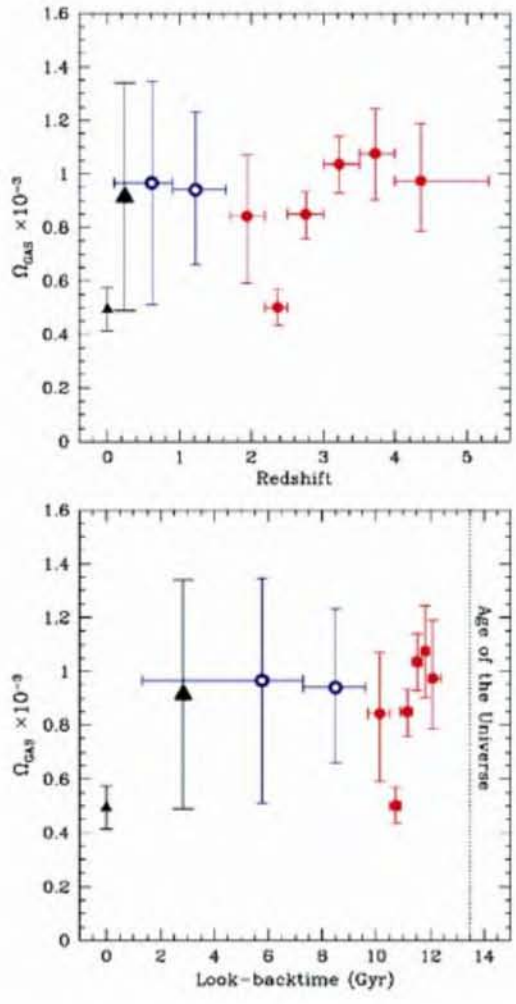

Figure 2. The evolution of the cosmic neutral gas density (Ω_{gas}) as a function of redshift and look back time (from ref. 8). The lowest redshift point[4] is based on the HIPASS blind HI 21 m survey, while the points above $z \sim 2$ are from ground based observations of damped Lyman-α systems. The intermediate redshift points are from HST observations of MgII selected systems and from GMRT radio observations The filled triangle is from GMRT observations of field galaxies at $z \sim 0.24$ (ref. 8). See ref. 8 for more details.

tings), Zwaan *et al.*[9] detected a single HI emission line, corresponding to an HI mass of $5.4 \pm 0.7 \times 10^9 h_{65}^{-2} M_\odot$. The HI detection was coincident with a galaxy pair. The spatial resolution was insufficient to determine if the galaxies were interacting. The observations also showed no evidence for interaction between the galaxy ISM and the cluster ICM. The HI mass inferred from the spectrum is consistent with that expected from a field pair, leading Zwaan *et al.*[9] to suggest that the detection corresponded to a field galaxy (pair) that was yet to fall into the cluster core. A much deeper survey was undertaken by Verheijen *et al.*[19], who observed two clusters A963 ($z \sim 0.206$) and A2192 ($z \sim 0.188$) with the upgraded WSRT. The two clusters were observed for 20×12 and 15×12 h respectively. A total of 42 galaxies were detected with HI masses ranging from 5×10^9 to $4 \times 10^{10} M_\odot$. The spatial distribution of the detected galaxies is shown in Figure 4. A963 is a dynamically relaxed looking cluster, and most of the detections come from a small group to the north-east of the cluster core. From the average redshifts of the detections, it appears that this group lies behind the cluster. A2192 is a less massive and more diffuse cluster, but even in this case, one can see that there is a paucity of detections in the cluster centre, and that most of the gas-rich galaxies lie in the periphery of the cluster. Thus, HI observations of clusters primarily provide information on the ongoing evolution of clusters and the galaxies that fall into them. This is of course, of interest in itself. It is unclear however, how (if at all) these results could be used to understand the evolution of typical field galaxies.

As mentioned above, cluster fields are popular targets for deep observations with synthesis telescopes because of the large number of galaxies that fall within the field of view. For single dish telescopes however, this is a disadvantage, since the large number of galaxies means that one cannot determine which galaxy is responsible for any detected emission. In the field however, particularly if the redshift distribution of galaxies is known, it may be possible to uniquely associate a given HI signal with a specific

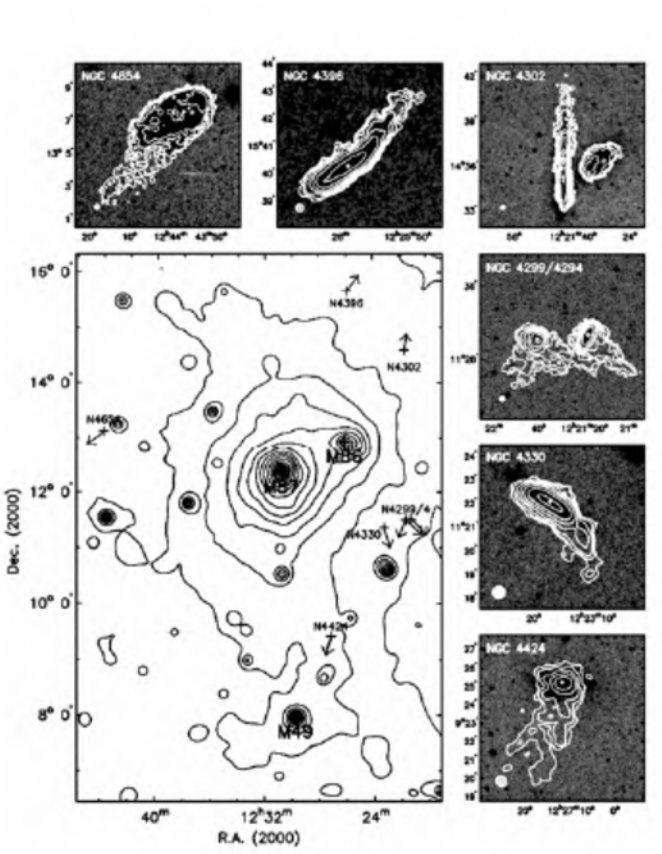

Figure 3. Montage of HI images of galaxies in the Virgo cluster (from ref. 15). The location of the galaxy relative to the cluster is shown in the central panel while the galaxy HI images themselves are shown in the surrounding panels. As expected from models in which interaction with the intracluster gas strips the galaxy ISM, the HI images show sharp edges towards the cluster centre and also long tails that point approximately away from the cluster centre. See ref. 15 for more details.

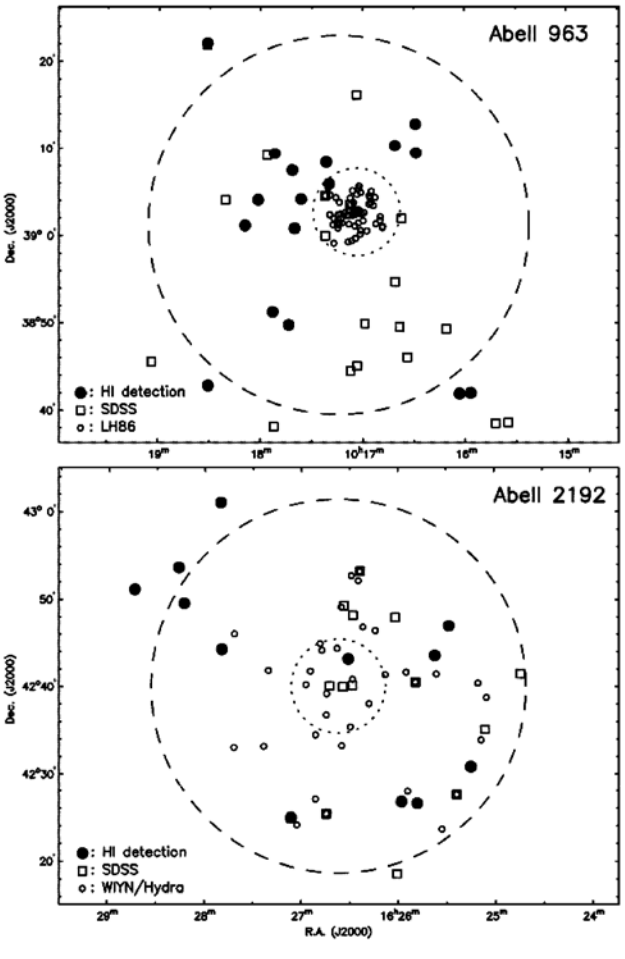

Figure 4. Distribution of the HI detections in the $z \sim 0.206$ and $z \sim 0.188$ clusters A963 and A2192 (from ref. 19). A963 is a dynamically relaxed looking cluster, and most of the gas rich galaxies are in a group that is located in the background of the cluster. A2192 is a less massive cluster, but even in this case, there are very few HI detections near the cluster core. The lack of HI-rich galaxies in the cluster cores is consistent with models in which galaxies that fall into the cluster rapidly lose their gas. See ref. 19 for more details.

galaxy. Catinella *et al.*[20] present results from pilot observations using the Arecibo radio telescope aimed at searching for HI from a carefully selected sample of isolated SDSS galaxies in the redshift range $0.17 \lesssim z \lesssim 0.25$. A total of 10 galaxies were detected. Not surprisingly these are relatively massive, gas-rich systems (HI mass in the range $3–8 \times 10^{10} M_{\odot}$ and HI to stellar mass ratios of 10−30%). Since comparable HI mass galaxies are rare at $z \sim 0$, there is no well matched reference sample that can be used as a baseline to check for evolutionary effects. Ongoing large scale HI surveys[21,22] are however expected to rectify this, and Arecibo observations look like a promising way to search for evolutionary effects in the most massive gas-rich galaxies.

To summarize, at current sensitivities, direct detections of HI gas in galaxies at redshifts as low as $z \sim 0.2$ is quite challenging. The relatively modest sensitivity of the current generation of radio telescopes limits one to being able to detect only the most massive galaxies, i.e. those that lie at the high mass edge of the HI mass function. An alternative approach would be to try and make a statistical detection of all the galaxies in the field of view. Assuming that the optical redshifts are known, the spectra at the relevant positions can be extracted from the HI data cube, aligned appropriately in redshift and co-added. Zwaan[23] demonstrated this technique for the ($z \sim 0.176$) cluster A2218, and showed that the galaxies in the cluster centre had an average HI mass of $\sim 3 \pm 1.2 \times 108\ h_{100}^{-2} M_{\odot}$. Similarly Chengalur *et al.*[24] in a proof of concept study of the $z \sim 0.06$ cluster A3128 with the ATCA reached an average HI mass sensitivity of $\sim 9 \times 10^8 M_{\odot}$ despite the modest sensitivity of ATCA and the relatively small (48 h) observation time. By dividing the galaxies within the field of view into sub-samples, one could identify the most gas-rich subset. The most gas-rich galaxies were found to lie in a group outside the cluster centre (see Figure 5).

The same technique was used by Lah *et al.*[8] to measure the atomic hydrogen gas content of star-forming galaxies at $z = 0.24$ (i.e. a look-back time of 3 Gyr). They used the GMRT to observe a sample of galaxies selected from Hα emitting field galaxies detected in a narrow-band imaging survey with the Subaru Telescope[25]. Since the Hα observations did not yield accurate enough redshifts for co-adding, the Anglo-Australian Telescope was used to obtain precise optical redshifts for the sample galaxies. A total of 121 galaxies lay within the GMRT spectral line data cube. From the co-added signal of these 121 galaxies, the average atomic hydrogen gas mass was measured to be $2.26 \pm 0.90 \times 10^9 M_{\odot}$. Since the area surveyed corresponded to an unbiased field region, it was possible to translate this HI signal into a cosmic density of neutral gas at $z = 0.24$, viz. $\Omega_{\rm gas} = 0.91 \pm 0.42 \times 10^{-3}$. This is the current highest redshift at which $\Omega_{\rm gas}$ has been constrained from 21-cm emission. The value obtained is consistent with that estimated from damped Lyman-α systems around this redshift (Figure 2). Lah *et al.*[8] also found that the relation between the Hα luminosity and the radio continuum luminosity and between the star formation rate (SFR) and the HI gas content in star-forming galaxies at $z = 0.24$ are the same as that expected from the correlations found at $z = 0$. The implication is that even though the average SFR is three times higher at $z = 0.24$ than at $z = 0$ (see Figure 1), the star formation mechanisms in field galaxies are not substantially different.

Absorption measurements

An alternative method for measuring the gas in collapsed objects at high redshifts is to look for the absorption lines that such a cloud would produce, were it to be like in front of a bright background source. This has the advantage that an absorption system sample constructed in this way would not be biased towards the most massive galaxies as an emission line survey inevitably is. This technique has been widely used, particularly to search for high redshift UV absorption lines that are redshifted to the wavelength range observable by ground based optical telescopes[26,27]. The most easily detected of these is the saturated Lyman-α absorption line. For even modest (i.e. few times 10^{19}) column densities of HI the optical depth is substantial even in the Lorenzian wings of the line. These very wide ('damped') profiles are easily detectable even in modest resolution spectra and are widely used to select samples of gas-rich collapsed objects in the distant universe. At column densities $\gtrsim 2 \times 10^{20}$, the bulk of the gas is neutral, and these systems, the so-called damped Lyman-α systems (or DLAs) are often regarded as the logical sites

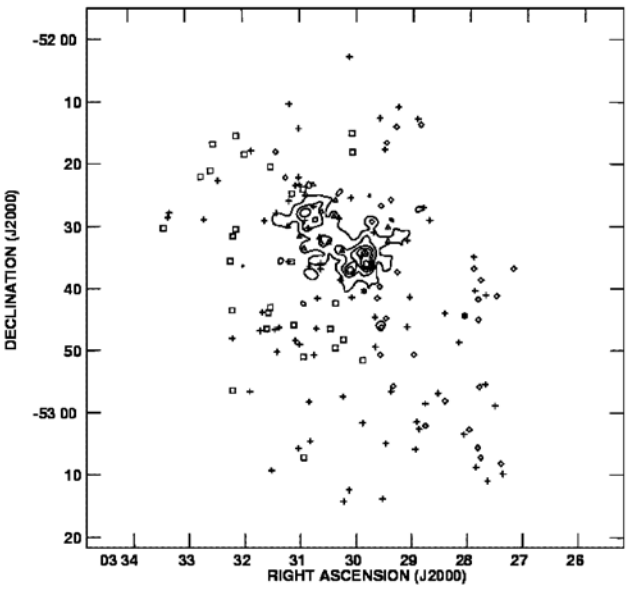

Figure 5. Gas-rich galaxies (as identified from co-adding the spectra of galaxies with known optical redshifts) in the galaxy cluster A3128. The gas-rich galaxies (shown as hollow squares) lie in a group on the outskirts of the cluster. See ref. 24 for more details.

for star formation in the distant universe, and hence, as precursors of the modern galaxies (see ref. 28 for a recent review).

Gas clouds which lie in front of radio loud quasars could give rise to absorption in the HI 21 cm line. Although radio observations of DLAs have been ongoing for several decades (e.g. ref. 29), there has been a recent revival in interest because of the expanded frequency coverage provided by the upgraded WSRT (e.g. ref. 30), the GMRT[31,32] and the GBT[33]. One of early drivers behind such observations was the possibility of measuring the spin temperature of the HI gas. The HI 21 cm line optical depth depends on both the gas column density and the spin temperature, i.e.

$$N_{\rm HI} = 1.823 \times 10^{18}\, T_{\rm spin} \int \tau(v)\, {\rm d}v, \qquad (1)$$

where $N_{\rm HI}$ is the gas column density in atoms cm^{-2}, $T_{\rm spin}$ the spin temperature of the gas and $\tau(v)$ the optical depth with v in km s^{-1}. In contrast, the Lyman-α optical depth depends only on the gas column density. A comparison of the gas column density derived from the Lyman-α observations with the 21 cm optical depth of the gas hence gives the average (strictly speaking, the column density weighted harmonic mean) spin temperature of the gas. This is interesting, because under many astrophysical conditions, the spin temperature of HI is the same as the kinetic temperature. Further, in models where the absorption comes from a two phase medium (i.e. the Cold Neutral Medium, CNM and the Warm Neutral Medium WNM, see e.g. ref. 34), the average spin temperature constrains the mass fraction of the gas in each phase. Assuming 80 and 8000 K as the typical temperatures of the CNM and WNM respectively, gas which is 50% CNM and 50% WNM would have an average spin temperature of 160 K, while gas which was 10% CNM and 90% WNM would have an average spin temperature of 735 K. The two phase model for the neutral atomic component of the ISM was developed in the context of the Milky Way (see the review by Kulkarni and Heiles[35]), and is still widely used, although there have been recent suggestions that a significant fraction of the HI is in a third, thermally unstable state (see refs 36 and 37). In the context of HI at cosmological redshifts, for at least two DLAs[38,39] (see also Figure 6) it has been established that the gas is in a two phase medium, with parameters similar to that in the Milky Way ISM. In two phase models, the deep narrow absorption components seen in most DLAs must arise from the CNM, since gas in the WNM phase generally has too low an optical depth to be observable at the current sensitivity levels. This means that the detection of a narrow HI 21 cm absorption line from a DLA essentially confirms the presence of cold HI gas in its ISM. This is in contrast to the highly saturated Lyman-α profile, which is insensitive to the temperature and kinematics of the absorbing gas.

The principal uncertainty in the measurement of $T_{\rm spin}$ is the spatial distribution of the absorbing gas. Equation (1) assumes that $N_{\rm HI}$ and $T_{\rm spin}$ are measured over the same region. In real life, this is not necessarily the case. The optical emission from quasars comes from an extremely compact region, substantially smaller than 1 AU across. The Lyman-α absorption hence traces the gas distribution along a narrow pencil beam through the cloud. In con-

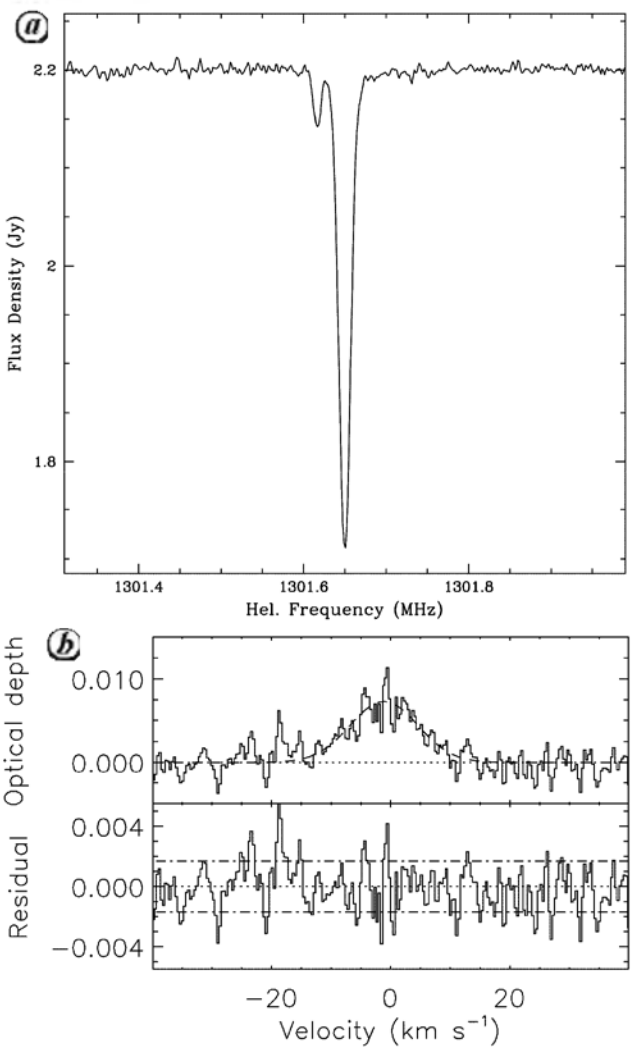

Figure 6. ***a***, The Arecibo HI 21 cm absorption spectrum from the $z \sim 0.0912$ absorber in front of the radio quasar B0738+313. The absorption consists of two deep narrow components and a wide, shallow component. The widths of the narrow components (which are upper limits to the kinetic temperature of the gas in these components) correspond to 297 ± 3 and 103 ± 10 K. These temperatures are too low to attribute to WNM gas, but are consistent with being CNM gas with a small contribution of non thermal motions to the line width. ***b***, The upper panel shows the residual spectrum after subtracting the narrow components, the lower panel shows the residuals after subtracting both the narrow and wide components. The wide component is interpreted as warm gas with kinetic temperature $<5050 \pm 950$ K. The total column density of gas computed using these temperatures is approximately equal to the column density derived from the damped Lyman-α profile, consistent with the idea that the HI in this absorber is in a two phase medium similar to that of the Milky Way ISM (from ref. 38).

trast, in lobe dominated radio sources, the radio emission could come from a region tens to hundreds of kpc in size. For such sources, the gas density along the radio and optical sightlines are completely uncorrelated. Such systems cannot be used for measuring T_{spin}. On the other hand, when the radio emission is core dominated, the gas density along the optical and radio sightlines are probably highly correlated. However, even in this situation, it is possible that the DLA obscures only a part of the background radio continuum. In order to determine the average spin temperature, one hence needs to either spatially resolve the 21 cm absorption (which is generally not possible with the current generation of radio telescopes), i.e. measure the 'covering factor', f (see ref. 40) or one needs to observe sources where the bulk of the radio emission from the background QSOs comes from a compact (on VLBI scales) core. In general, therefore the relation between the Lyman-α measured N_{HI}, and the radio measured T_{spin} is

$$N_{HI} = \frac{1.823 \times 10^{18} T_{spin}}{f} \int \tau(v)\, dv, \qquad (2)$$

where f is the fraction of the radio continuum that is covered by the absorbing gas, and the further assumption that the N_{HI} measured along the line of sight to the quasar applies the entire absorber has been made. Figure 7 shows a recent compilation of the spin temperature in DLAs as a function of the redshift. As can be seen, high- and low-spin temperatures are seen at low and intermediate redshifts, whereas the bulk of the gas at high redshifts is at high-spin temperatures. The dividing line between 'high' and 'low' spin temperatures is taken to be 300 K, more than 90% of the lines of sight through the Milky Way and in nearby spirals have average spin temperature less than 300 K (ref. 41). The tendency for high redshift absorbers to have high-spin temperatures has been noted earlier by, among others[37,42]. One possible explanation for this is that high redshift systems have lower metallicities, and are also likely to be of smaller mass and have lower mid plane pressure (e.g. ref. 43). All of these factors inhibit the formation of the CNM. Of course, as discussed above (see also ref. 44), for many of these systems the covering factor has not been directly measured, and hence it remains a possibility that the high-spin temperatures are not real, but are an artefact arising from an over estimation of the covering factor. There have even been suggestions that the covering factor could evolve systematically with redshift, with high redshift systems having low covering factors (see ref. 45). This would reproduce the trend seen in Figure 7 without any actual evolution of the average T_{spin} with redshift. However, recent VLBI measurements[46] indicate that no such evolution of the covering factor is observed. For 24 DLAs, for which the covering factor was estimated using VLBI observations 14 DLAs with at $z > 1.5$ have covering factors $f \sim 0.45$–1, while 10 DLAs at $z < 1$ have $f \sim 0.41$–1. The distribution of covering factors for the high and low redshift subsamples are statistically indistinguishable. On the face of it, the implication of Figure 7 is that high redshift DLAs are WNM dominated. The low CNM fractions deduced from the radio observations, are in contradiction to the modeling of the star formation rate (as inferred from the CII* absorption) in DLAs. These models suggest that a low CNM fraction would lead to unrealistically high star formation rates[47]. In contrast to the typical high-spin temperatures seen at high redshifts, both low and high-spin temperatures are seen at low redshifts, implying that at least some low redshift systems have a substantial CNM fraction. Further, from a search for HI 21 cm absorption in MgII selected systems[48], show that the probability of detecting HI 21 cm in MgII selected systems at $z \sim 1$ is, within the error bars, the same as at low redshifts. This suggests that most gas-rich galaxies contain significant amounts of cold gas by $z \sim 1$ (see also ref. 49). The sample sizes are still small however, and confirmation of these trends from observations of larger samples is critical.

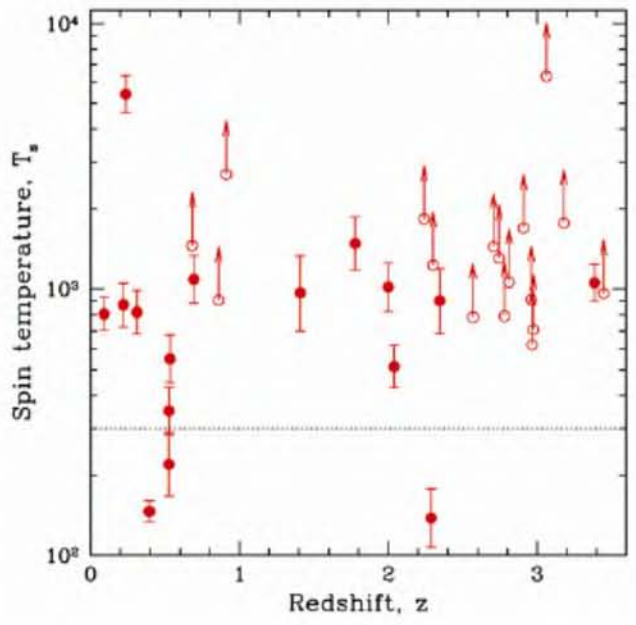

Figure 7. A plot of spin temperature T_{spin} as a function of redshift for all DLAs for which measurements are available (from ref. 50). The horizontal line is at 300 K, more than 90% of the lines of sight through the milkyway have temperatures below this value[41]. As can be seen both high- and low-spin temperatures are seen at low redshifts, while high redshift absorbers tend to have high-spin temperatures.

For objects that lie in front of extended radio sources, it is possible (given sufficient angular resolution) to directly image the distribution and kinematics of the absorbing gas[51]. Since the strength of the absorption depends on the physical parameters (i.e. N_{HI}, T_{spin}) of the absorber and the strength of the background source, it is independent of redshift. Detection of 21 cm absorption thus provides

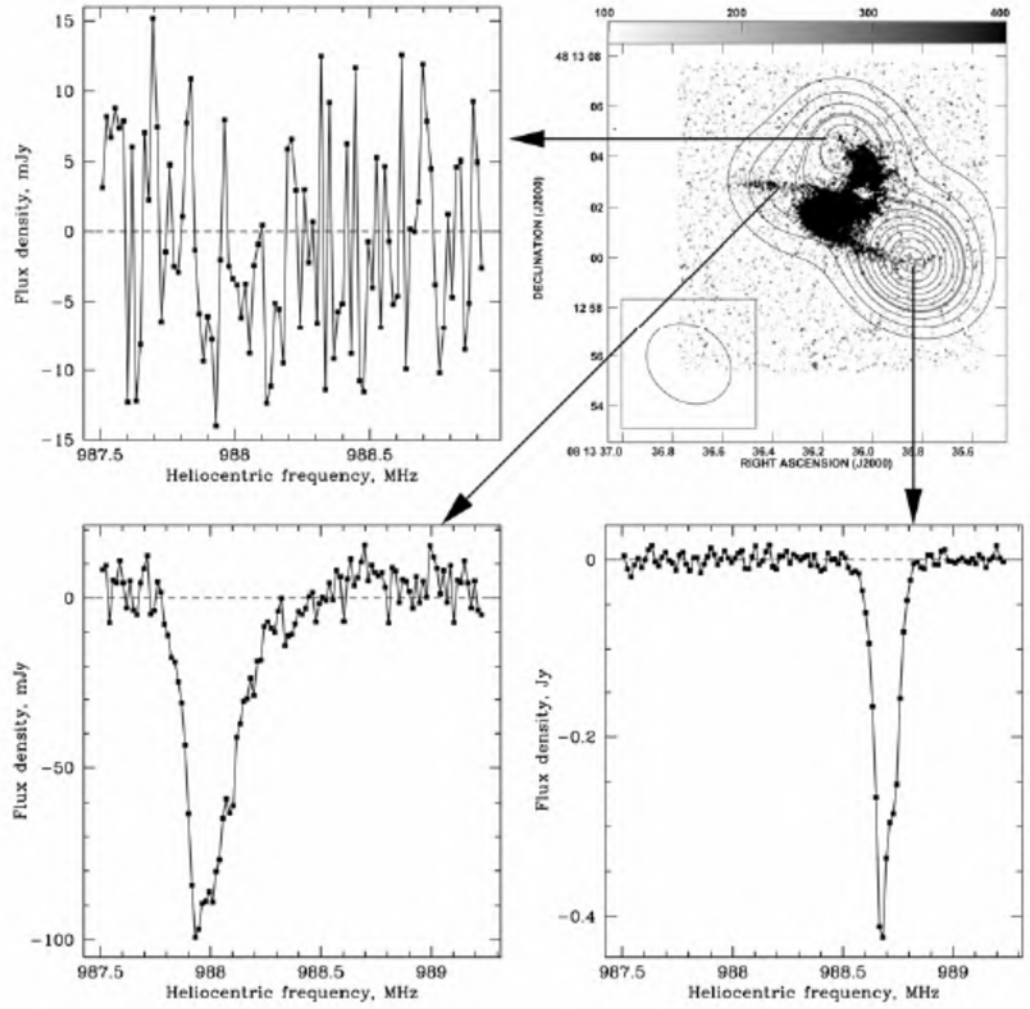

Figure 8. Spatially resolved HI 21 cm absorption from the $z \sim 0.437$ absorber towards 3C196 (from ref. 52). The observations clearly show that the deep absorption comes from the dense gas along the spiral arms, and also allows one to make a crude velocity field of the absorbing gas.

an exciting means of observing the gas kinematics in collapsed objects at high redshifts. Figure 8 shows GMRT images of the absorption arising from the spiral galaxy at redshift $z \sim 0.437$ that lies in front of the radio galaxy 3C196 (ref. 52). The observations clearly show that the deep absorption comes from dense gas along the spiral arms (see also ref. 53), and also allows one to make a crude velocity field of the absorbing gas.

Observations of the precise redshift of spectral lines from high redshift DLAs can also be used to check if the values of the fundamental constants change with time. Although the suggestion that the values of certain fundamental constants may evolve with cosmic time is relatively old[54], interest in this possibility has been reignited by claims that the fine structure constant α evolves with redshift[55,56]. On the theoretical front, such variations are expected in extra-dimensional theories like the Kaluza-Klein theories and superstring theories. In these theories, the values of the coupling ('fundamental') constants depend on the expectation values of some cosmological scalar fields. Changes in the values of the coupling constants are thus to be expected if this field varies with location and time. Different coupling constants (such as α, the proton g-factor g_p, the electron–proton mass ratio $\mu \equiv m_e/m_p$, the gravitational constant G, etc.) could, in principle, vary simultaneously. For example, Calmet and Fritzsch[57] and Langacker *et al.*[58] found that variations in the value of α should be accompanied by much larger changes (by ~2 orders of magnitude) in the value of μ. Reviews of the available experimental and observational measurements on the variability of the coupling constants can be found in refs 59–61.

The HI 21 cm line is a hyperfine transition. A comparison of the observed redshift of the line, with the observed fine structure redshift of e.g. MgII lines allows one to constrain variations in $\alpha^2 g_p \mu$, where g_p is the electron gyro-magnetic ratio, α the fine structure constant and μ the electron to proton mass ratio (see ref. 62). One impor-

tant caveat is that this comparison assumes that the two absorption lines arise in the same gas, i.e. that there is no relative motion (and hence no relative Doppler shift) between the gas that gives rise to the MgII absorption and the 21 cm absorption. Since it is difficult to rule out a priori, the best one can do is to observe a large sample of absorbers and assume that on the average the doppler shift between these two absorbing species is zero[63]. Figure 9 shows a specific case with clear velocity offsets between the HI 21 cm and optical absorption.

Similarly a comparison of mm wavelength rotational transitions and the HI 21 cm hyperfine transition has been used to constraint variations in the product[65] $g_p\alpha^2$. High resolution (VLBI) observations have also been used to try and closely align the HI 21 cm and molecular line absorptions and hence minimize the possibility of the absorption arising in different gas clouds[66]. Another set of interesting low frequency spectral lines that have recently been detected in absorption at cosmological redshifts[67,68] are the 18 cm lines from the OH molecule. The ground state of the OH molecule is split into four levels by Λ doubling and the hyperfine interaction. The exact frequencies of these lines hence depends on the electron to proton mass ratio μ in addition to g_p and the fine structure constant α. Chengalur and Kanekar[69] show that a comparison of the redshifts of the OH main lines with the redshifts of the HI 21 cm line and the CO rotational lines allows one to simultaneously constrain all three of g_p, α and μ, although the constraints are rather weak unless one assumes (as is often done, e.g. ref. 66, see also refs 58 and 70) that the variation is g_p are small and can be ignored. Alternatively, if the higher frequency OH lines (e.g. those near $\lambda \sim 6$ cm) were also to be detected in an object at cosmological redshifts, one could (under the assumption that g_p and μ are constant) use the OH transitions alone to place constraints on the variation[71] in α, or joint constraints if one allows the possibility of a change in the value of all of these constants[72]. A more interesting situation is shown in Figure 10 (see refs 73 and 74) which shows the 1612 and 1720 MHz OH satellite lines from the associated absorber PKS1413+135. The two lines can be seen to be conjugate, i.e. the 1612 line is in absorption when the 1720 is in emission and vice versa. This conjugate behaviour holds across the spectrum, and as can be seen in Figure 10 the sum of the two spectra is consistent with noise. This behavior can be understood as a consequence of 'competitive gain' of the two possible rotational ladders along which the OH molecule, once excited, can cascade down to the ground state. Similar conjugate spectra have been observed in molecular clouds in our own galaxy as well as in the nearby radio galaxy Centaurus A[75]. A consequence of this conjugate behaviour is that it is guaranteed that the 1612 and 1720 MHz lines arise from the

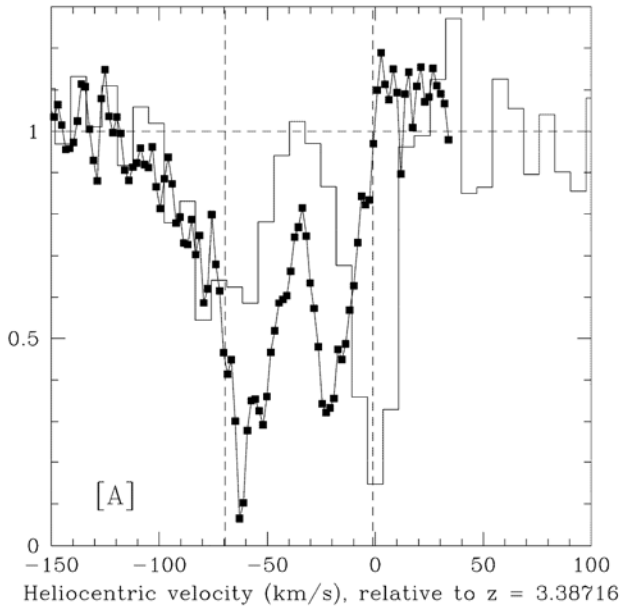

Figure 9. The HI 21 cm absorption spectrum from the $z \sim 3.3$ absorber towards PKS 0201+113. The HI 21 cm spectrum (from ref. 64) is shown as a histogram, while the FeIIλ1122 Keck Hires spectrum is shown as solid squares. The dashed vertical lines show the measured redshifts of the HI 21 cm absorption components. There is a clear offset between the metal line and HI 21 cm absorption (see ref. 64 for more details).

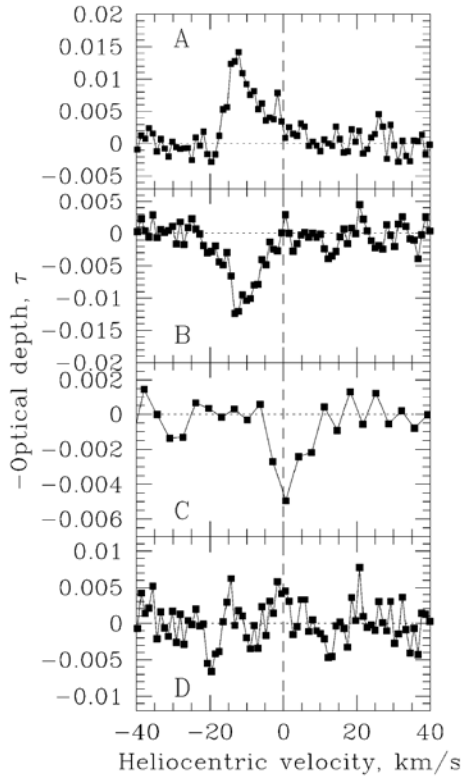

Figure 10. Optical depth spectra of the OH lines observed towards PKS 1413+135 (from ref. 74). The heliocentric velocity has been computed relative to $z = 0.24671$. Note that the 1720 and 1612 MHz satellite lines (top two panels) are exactly conjugate, and their sum is consistent with noise (bottom panel). This allows one to constrain variations in $g_p[\alpha^2/\mu]^{1.89}$ where $\mu = m_e/m_p$. See ref. 74 for more details.

same gas, without any relative Doppler shift. Further, since the line shapes are identical, any small shifts between them can be determined using non-parametric methods (e.g. a cross correlation analysis) instead of the usual method of locating the peak via template fitting (e.g. assuming that the line profile is a Gaussian, or a sum of Gaussians). Comparison between these two lines constrains the value of $G = g_p[\alpha^2/\mu]^{1.89}$ where $\mu = m_e/m_p$ within even a single system free of systematic effects. Observations of the $z \sim 0.247$ absorber towards[74] PKS 1413+135 constrain $\Delta G/G = 2.2 \pm 3.810^{-5}$. A comparison of the HI and OH absorption line redshifts of the $z \sim 0.765$ gravitational lens toward PMN J0134-0931 constrain $\Delta F/F = (0.44 \pm 0.36$ (stat) $\pm$ 1.0 (syst) $\times 10^{-5}$, where $F = g_p[\alpha^2/\mu]^{1.57}$ (ref. 76).

Future prospects

A continuing theme in this article (see earlier section), is that the detection of HI in emission is sensitivity limited. To explore the high redshift universe will require substantially more sensitivity than is provided by the current generation of radio telescopes. In fact, a major science driver behind both the proposed SKAs as well as the next generation radio telescopes, viz. the Australian ASKAP and the South African Meerkat is to greatly extend the redshift range to which observations of HI emission from galaxies is possible.

The sensitivity, field of view and instantaneous bandwidth of the SKA are all likely to be more than an order of magnitude higher than that of the current radio telescopes[77]. The combination of these factors will lead to a transformative change in our ability to study HI at high redshifts. Redshift surveys could be done up to redshifts $z \sim 1.5$. Since the HI is optically thin, a redshift survey automatically also yields the total HI mass and the HI kinematic velocity spread). Statistical studies of the HI content of galaxies[78,79], its connection to star formation, etc. could be done for $0 < z \lesssim 3$.

The ASKAP will consist of up to 45 dishes, each 12 m in diameter, and with an instantaneous field of view of 30 deg^2 and an instantaneous bandwidth[80] of 300 MHz. Thus while the total collecting area is modest, the combination of large instantaneous bandwidth and field of view make it an extremely efficient survey telescope. Johnston *et al.*[80] estimate that its survey speed will be more than an order of magnitude larger than that of the existing radio telescopes. Proposed surveys using this telescope include a shallow hemispheric survey that would in a total of one year's observing time reach a depth of $z \sim 0.05$ for HI emission, and detect the most massive galaxies to $z \sim 0.15$. A deep (i.e. one year) integration in a single field of view is estimated to detect $\sim 10^5$ galaxies, with typical depth $z \sim 0.2$ but with the most massive galaxies being detected[80] to $z \sim 0.7$. Such surveys would provide accurate measurements of Ω_{gas} as a function of redshift, as well as provide unique inputs into understanding galaxy formation and evolution.

As discussed earlier, the range of redshifts to which HI can be detected can be substantially extended by stacking together the spectra of galaxies whose redshifts are known. This has the further advantage of yielding a sample for which one can directly relate the gas content to other important quantities, e.g. the spectral type of the galaxy, SFR, environmental dependence of the gas content etc. There are several ongoing redshift surveys that will yield samples that are ideal for follow-up in stacking experiments. For example, the WiggleZ survey (which covers seven fields, each of area >100 deg^2), the zCosmos field, the Chandra Deep Field (South), etc. will all provide redshifts useful for stacking. The WiggleZ survey is expected to measure 200,000 redshifts in a total area >700 deg^2 by 2010. Figure 11 shows the expected co-added signal in a single 30 deg^2 ASKAP field of view after a 1000 h integration using only the redshifts that are currently available. The red dashed line shows the average HI mass in galaxies at $0.5 < z < 1$ required to obtain a 5σ co-added detection on stacking the HI emission from individual galaxies[82]. The solid line with error bars shows the expected HI signal from the galaxies for which redshifts are currently available, and further assuming that the HI mass function is as measured at $z \sim 0$ by Zwaan *et al.*[4]. As can be seen, even in this conservative scenario, one would expect to make a measurement of the average HI content of star forming galaxies out to $z \sim 1$. The sensitivity in a ~5000 h observation, should be sufficient to obtain a dust bias independent measurement of the

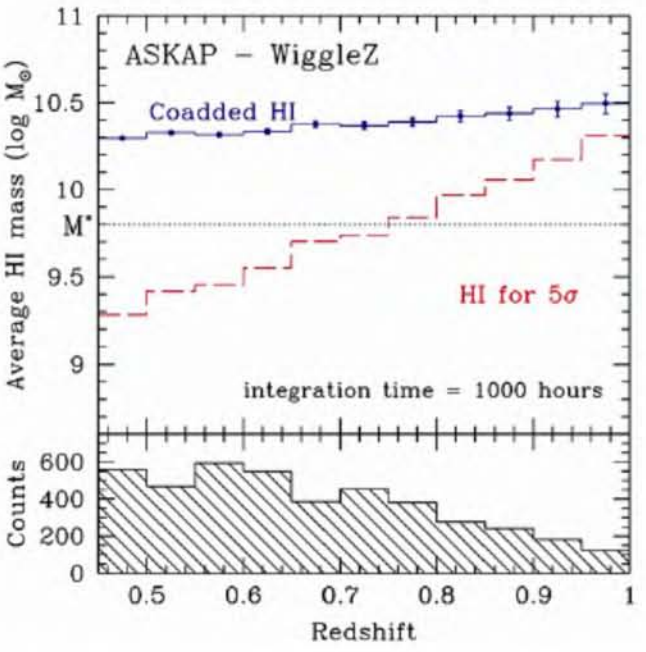

Figure 11. The average HI mass detectable in an emission stacking experiment, assuming a 1000 h ASKAP integration and stacking ~5000 galaxies from the WiggleZ survey.

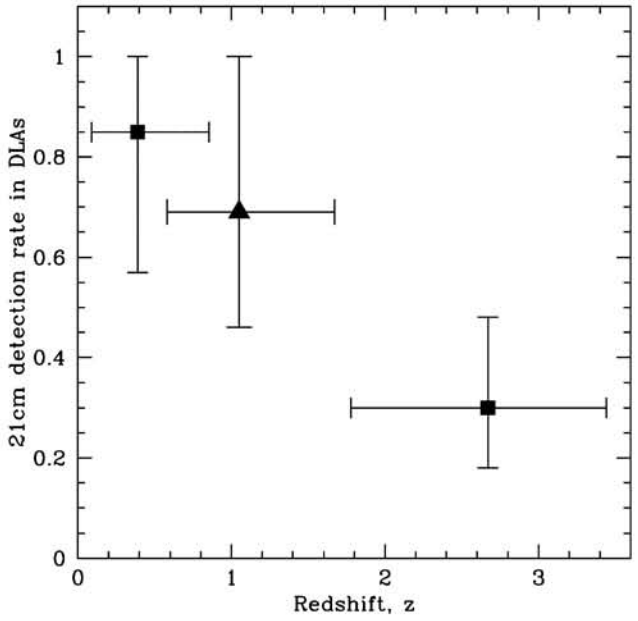

Figure 12. The detection rate of HI 21 cm absorption in DLAs as a function of redshift. At $z \lesssim 1$ the detection rate is ≳70%. From ref. 48.

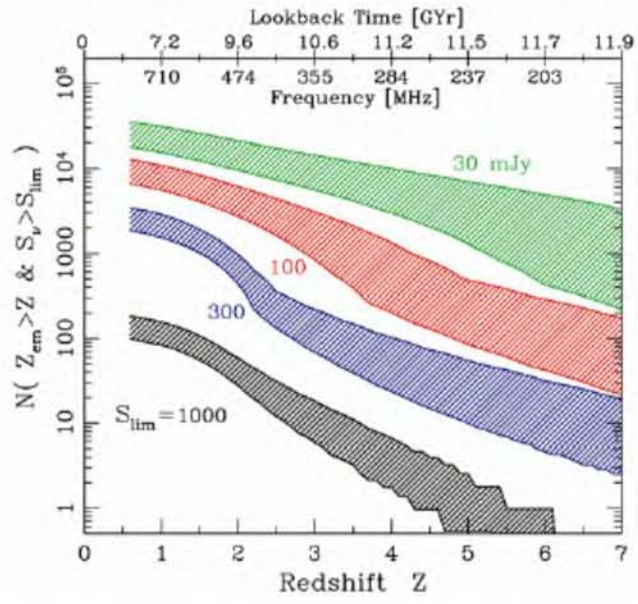

Figure 13. The number of radio galaxies with flux densities greater than some threshold (30, 100, 300, 1000 mJy) and redshifts above some redshift z. From ref. 81.

cosmic neutral gas density at $0.5 < z < 1$, as well as to probe the average HI mass of galaxies of different morphological types and in different environments.

ASKAP will also be an excellent facility for a blind search for HI absorption against bright radio sources. Such a search is interesting because, among other things, it will yield estimates of $\Omega_{\rm gas}$ independent of the detection of the Lyman-α absorption. It has long been a matter of debate whether the current DLA based estimates of $\Omega_{\rm gas}$ are biased to exclude dusty absorbers (which being optically thick at UV wavelengths obscure the back-ground quasar). For example, Ellison *et al.*[83] estimates that roughly half the DLAs at $z \sim 2.5$ could be missed in optically-selected samples due to dust obscuration of the background quasars. This fraction is likely to be significantly higher at $z \sim 1$, given the copious amounts of dust found in Spitzer-selected samples (see e.g. ref. 84).

Figure 12 shows the detection rate of HI 21 cm absorption in DLAs (from ref. 48) at a 3σ optical depth sensitivity of ~0.013 per ~10 km/s. As can be seen, the detection rate of HI 21 cm absorption in DLAs is quite high at $z \lesssim 1$; $n_{21{\rm cm,DLA}} \gtrsim 0.7$. Figure 13 (from ref. 74) shows the number of radio galaxies over 2π steradians plotted as a function of redshift. The separate curves are for flux density cut-offs of 30, 100, 300 and 1000 mJy respectively. Putting the information in these two plots together, one would predict that observations ~100 ASKAP fields, with a 50 h integration per field, would yield ≳250 new HI 21 cm absorbers at $0.5 < z < 1.0$. The sensitivity of a 50 h integration is also such that one would be able to detect all OH absorbers (with OH column density and excitation temperature similar to those currently known), with $0.7 \lesssim z \lesssim 1.4$ towards sources with $S_{700} \gtrsim 100$ mJy.

Although the Meerkat has a smaller field of view, it will also be an excellent instrument for such studies, as will the EVLA and the upgraded GMRT, and a focal plane array equipped WSRT[85]. For radio observations of the HI 21 cm line, the future holds the prospect of moving from fasting to feasting.

1. White, S. D. M. and Rees, M. J., *MNRAS*, 1978, **183**, 341.
2. Baan, W. A., *Nature*, 1985, **315**, 26.
3. Darling, J., *ApJL*, 2007, **669**, L9.
4. Zwaan, M. A., Meyer, M. J., Staveley-Smith, L. and Webster, R. L., *MNRAS*, 2005, **359**, L30; arXiv:astroph/0502257.
5. Lilly, S. J., Le Fevre, O., Hammer, F. and Crampton, D., *ApJL*, 1996, **460**, L1+, arXiv:astro-ph/9601050.
6. Madau, P., Ferguson, H. C., Dickinson, M. E., Giavalisco, M., Steidel, C. C. and Fruchter, A., *MNRAS*, 1996, **283**, 1388; arXiv: astro-ph/9607172.
7. Hopkins, A. M. and Beacom, J. F., *ApJ*, 2006, **651**, 142; arXiv: astro-ph/0601463.
8. Lah, P. *et al.*, *MNRAS*, 2007, **376**, 1357; arXiv:astro-ph/0701668.
9. Zwaan, M. A., van Dokkum, P. G. and Verheijen, M. A. W., *Science*, 2001, **293**, 1800; arXiv:astro-ph/0109108.
10. Gunn, J. E. and Gott, J. R. I., *ApJ*, 1972, **176**, 1.
11. Quilis, V., Moore, B. and Bower, R., *Science*, 2000, **288**, 1617; arXiv:astro-ph/0006031.
12. Moore, B., Katz, N., Lake, G., Dressler, A. and Oemler, A., *Nature*, 1996, **379**, 613; arXiv:astro-ph/9510034.
13. Bekki, K., *ApJL*, 1999, **510**, L15; arXiv:astroph/9811117.
14. Cayatte, V., van Gorkom, J. H., Balkowski, C. and Kotanyi, C., *AJ*, 1990, **100**, 604.
15. Chung, A., van Gorkom, J. H., Kenney, J. D. P. and Vollmer, B., *ApJL*, 2007, **659**, L115; arXiv:astroph/0703338.
16. Dressler, A., *ApJ*, 1980, **236**, 351.
17. Giovanelli, R. and Haynes, M. P., *ApJ*, 1985, **292**, 404.
18. Solanes, J. M., Manrique, A., García-Gómez, C., González-Casado, G., Giovanelli, R. and Haynes, M. P., *ApJ*, 2001, **548**, 97; arXiv:astro-ph/0007402.
19. Verheijen, M., van Gorkom, J. H., Szomoru, A., Dwarakanath, K. S., Poggianti, B. M. and Schiminovich, D., *ApJL*, 2007, **668**, L9.

20. Catinella, B., Haynes, M. P., Giovanelli, R., Gardner, J. P. and Connolly, A. J., *ApJL*, 2008, **685**, L13.
21. Giovanelli, R. *et al.*, *AJ*, 2005, **130**, 2613; arXiv:astro-ph/0508300.
22. Freudling, W. *et al.*, In *The Evolution of Galaxies Through the Neutral Hydrogen Window* (eds Minchin, R. and Momjian, E.), American Institute of Physics Conference Series, 2008, vol. 1035, pp. 242–245.
23. Zwaan, M. A., Ph D thesis, Groningen University, 2000.
24. Chengalur, J. N., Braun, R. and Wieringa, M., *A&A*, 2001, **372**, 768; arXiv:astro-ph/0104331.
25. Fujita, S. S. *et al.*, *ApJL*, 2003, **586**, L115; arXiv:astroph/0302473.
26. Wolfe, A. M., Turnshek, D. A., Smith, H. E. and Cohen, R. D., *ApJS*, 1986, **61**, 249.
27. Prochaska, J. X., Herbert-Fort, S. and Wolfe, A. M., *ApJ*, 2005, **635**, 123; arXiv:astro-ph/0508361.
28. Wolfe, A. M., Gawiser, E. and Prochaska, J. X., *ARAA*, 2005, **43**, 861; arXiv:astro-ph/0509481.
29. Roberts, M. S., Brown, R. L., Brundage, W. D., Rots, A. H., Haynes, M. P. and Wolfe, A. M., *AJ*, 1976, **81**, 293.
30. Lane, W. M., Briggs, F. H. and Smette, A., *ApJ*, 2000, **532**, 146; arXiv:astro-ph/9911142.
31. Chengalur, J. N. and Kanekar, N., *MNRAS*, 1999, **302**, L29.
32. Kanekar, N., Ph D thesis, Pune University, 2000.
33. Darling, J., Giovanelli, R., Haynes, M. P., Bolatto, A. D. and Bower, G. C., *ApJL*, 2004, **613**, L101; arXiv:astroph/0408531.
34. Wolfire, M. G., McKee, C. F., Hollenbach, D. and Tielens, A. G. G. M., *ApJ*, 2003, **587**, 278; arXiv:astroph/0207098.
35. Kulkarni, S. and Heiles, C., In *Galactic and Extra Galactic Radio Astronomy*, 1988.
36. Heiles, C. and Troland, T. H., *ApJ*, 2003, **586**, 1067; arXiv:astro-ph/0207105.
37. Kanekar, N. and Chengalur, J. N., *A&A*, 2003, **399**, 857; arXiv:astro-ph/0211637.
38. Lane, W., Ph D thesis, University of Groningen, 2000.
39. Kanekar, N., Ghosh, T. and Chengalur, J. N., *A&A*, 2001, **373**, 394; arXiv:astro-ph/0104321.
40. Briggs, F. H. and Wolfe, A. M., *ApJ*, 1983, **268**, 76.
41. Braun, R. and Walterbos, R. A. M., *ApJ*, 1992, **386**, 120.
42. Carilli, C. L., Lane, W., de Bruyn, A. G., Braun, R. and Miley, G. K., *AJ*, 1996, **111**, 1830, 1996.
43. Chengalur, J. N. and Kanekar, N., *MNRAS*, 2000, **318**, 303; arXiv:astro-ph/0011540.
44. Curran, S. J., Murphy, M. T., Pihlström, Y. M., Webb, J. K. and Purcell, C. R., *MNRAS*, 2005, **356**, 1509; arXiv:astro-ph/0410647.
45. Curran, S. J. and Webb, J. K., *MNRAS*, 2006, **371**, 356; arXiv:astro-ph/0606180.
46. Kanekar, N., Lane, W. M., Momjian, E., Briggs, F. H. and Chengalur, J. N., *MNRAS*, 2009, **394**, L61, 0903.4483.
47. Wolfe, A. M., Prochaska, J. X. and Gawiser, E., *ApJ*, 2003, **593**, 215; arXiv:astro-ph/0304040.
48. Kanekar, N., Prochaska, J. X., Ellison, S. L. and Chengalur, J. N., ArXiv e-prints, 2009, 0903.4487.
49. Gupta, N., Srianand, R., Petitjean, P., Khare, P., Saikia, D. J. and York, D. G., *ApJL*, 2007, **654**, L111; arXiv:astro-ph/0611836.
50. Kanekar, N. *et al.* (in preparation) (2009).
51. Briggs, F. H., Wolfe, A. M., Liszt, H. S., Davis, M. M. and Turner, K. L., *APJ*, 1989, **341**, 650.
52. Kanekar, N. and Chengalur, J. N. (in preparation) (2009).
53. Briggs, F. H., de Bruyn, A. G. and Vermeulen, R. C., *A&A*, 2001, **373**, 113; arXiv:astro-ph/0104457.
54. Dirac, P. A. M., *Nature*, 1961, **192**, 441.
55. Webb, J. K., Flambaum, V. V., Churchill, C. W., Drinkwater, M. J. and Barrow, J. D., *Phys. Rev. Lett.*, 1999, **82**, 884.
56. Webb, J. K. *et al.*, *Phys. Rev. Lett.*, 2001, **87**, 091301.
57. Calmet, X. and Fritzsch, H., *Phys. Lett.*, 2002, **B540**, 173.
58. Langacker, P., Segrè, G. and Strassler, M. J., *Phys. Lett.*, 2002, **B528**, 121; arXiv:hep-ph/0112233.
59. Uzan, J.-P., *Rev. Mod. Phys.*, 2003, **75**, 403.
60. García-Berro, E., Isern, J. and Kubyshin, Y. A., *A&A Rev.*, 2007, **14**, 113.
61. Kanekar, N., *Modern Phys. Lett.*, 2008, **A23**, 2711; 0810.1356.
62. Wolfe, A. M., Brown, R. L. and Roberts, M. S., *Phys. Rev. Lett.*, 1976, **37**, 179.
63. Tzanavaris, P., Murphy, M. T., Webb, J. K., Flambaum, V. V. and Curran, S. J., *MNRAS*, 2007, **374**, 634; arXiv:astro-ph/0610326.
64. Kanekar, N., Chengalur, J. N. and Lane, W. M., *MNRAS*, 2007, **375**, 1528; arXiv:astro-ph/0701074.
65. Drinkwater, M. J., Webb, J. K., Barrow, J. D. and Flambaum, V. V., *MNRAS*, 1998, **295**, 457; arXiv:astroph/9711290.
66. Carilli, C. L. *et al.*, *Phys. Rev. Lett.*, 2000, **85**, 5511; arXiv:astro-ph/0010361.
67. Chengalur, J. N., de Bruyn, A. G. and Narasimha, D., *A&A*, 1999, **343**, L79; arXiv:astro-ph/9904055.
68. Kanekar, N. and Chengalur, J. N., *A&A*, 2002, **381**, L73; arXiv:astro-ph/0111563.
69. Chengalur, J. N. and Kanekar, N., *Phys. Rev. Lett.*, 2003, **91**, 241302; arXiv:astro-ph/0310764.
70. Flambaum, V. V., Leinweber, D. B., Thomas, A. W. and Young, R. D., *Phys. Rev.*, 2004, **D69**, 115006; arXiv:hepph/0402098.
71. Darling, J., *Phys. Rev. Lett.*, 2003, **91**, 011301; arXiv:astro-ph/0305550.
72. Kanekar, N. and Chengalur, J. N., *MNRAS*, 2004, **350**, L17; arXiv:astro-ph/0310765.
73. Darling, J., *ApJ*, 2004, **612**, 58; arXiv:astro-ph/0405240.
74. Kanekar, N., Chengalur, J. N. and Ghosh, T., *Phys. Rev. Lett.*, 2004, **93**, 051302; arXiv:astro-ph/0406121.
75. van Langevelde, H. J., van Dishoeck, E. F., Sevenster, M. N. and Israel, F. P., *ApJL*, 1995, **448**, L123+.
76. Kanekar, N. *et al.*, *Phys. Rev. Lett.*, 2005, **95**, 261301; arXiv:astro-ph/0510760.
77. Schilizzi, R. *et al.*, SKA Memo 100, 2007.
78. van der Hulst, J. M., Sadler, E. M., Jackson, C. A., Hunt, L. K., Verheijen, M. and van Gorkom, J. H., *New Astron. Rev.*, 2004, **48**, 1221; arXiv:astro-ph/0411058.
79. Rawlings, S., Abdalla, F. B., Bridle, S. L., Blake, C. A., Baugh, C. M., Greenhill, L. J. and van der Hulst, J. M., *New Astron. Rev.*, 2004, **48**, 1013; arXiv:astroph/0409479.
80. Johnston, S. *et al.*, *Exp. Astron.*, 2008, **22**, 151, 0810.5187.
81. Kanekar, N. and Briggs, F. H., *New Astron. Rev.*, 2004, **48**, 1259; arXiv:astro-ph/0409169.
82. Lah, P., Ph D thesis, Australia National University, 2009.
83. Ellison, S. L., Yan, L., Hook, I. M., Pettini, M., Wall, J. V. and Shaver, P., *A&A*, 2001, **379**, 393; arXiv:astroph/0109205.
84. Verma, A., Charmandaris, V., Klaas, U., Lutz, D. and Haas, M., *Space Sci. Rev.*, 2005, **119**, 355; arXiv:astro-ph/0507165.
85. Verheijen, M. A. W., Oosterloo, T. A., van Cappellen, W. A., Bakker, L., Ivashina, M. V. and van der Hulst, J. M., In *The Evolution of Galaxies Through the Neutral Hydrogen Window* (eds Minchin, R. and Momjian, E.), American Institute of Physics Conference Series, 2008, vol. 1035, pp. 265–271.

ACKNOWLEDGEMENTS. I am grateful to Nissim Kanekar and Philip Lah for allowing me to use data and figures prior to publication, and to Nissim Kanekar for a careful reading of the manuscript and several useful comments.